

Laser Surface Treatment of Hydro and Thermal Power Plant Components and Their Coatings: A Review and Recent Findings

B.S. Mann

(Submitted April 16, 2015; in revised form July 29, 2015; published online September 2, 2015)

High-power diode laser (HPDL) surface modification of hydro and thermal power plant components is of the utmost importance to minimize their damages occurring due to cavitation erosion, water droplet erosion, and particle erosion (CE, WDE, and PE). Special emphasis is given on the HPDL surface treatment of martensitic and precipitate-hardened stainless steels, Ti6Al4V alloy, plasma ion nitro-carburized layers, high pressure high velocity oxy-fuel and twin-wire arc sprayed coatings. WDE test results of all these materials and coatings in 'untreated' and 'HPDL- treated at 1550 °C' conditions, up to 8.55 million cycles, are already available. Their WDE testing was further continued up to 10.43 million cycles. The X20Cr13 and X10CrNiMoV1222, the most common martensitic stainless steels used in hydro and thermal power plants, were HPDL surface treated at higher temperature (1650 °C) and their WDE test results were also obtained up to 10.43 million cycles. It is observed that the increased HPDL surface temperature from 1550 to 1650 °C has resulted in significant improvement in their WDE resistances because of increased martensitic (α') phase at higher temperature. After conducting long-range WDE tests, the correlation of CE, WDE, and PE resistances of these materials and protective coatings with their mechanical properties such as fracture toughness and microhardness product, ultimate resilience, modified resilience, and ultimate modified resilience has been reviewed and discussed. One of the edges of a 500 MW low pressure steam turbine moving blade (X10CrNiMoV1222 stainless steel) was HPDL surface treated at 1550 °C and its radii of curvatures and deflections were measured. These were compared with the data available earlier from a flat rectangular sample of similar composition and identical HPDL surface temperature.

Keywords cavitation erosion, diode laser, hydro and thermal power plants, particle erosion, plasma ion nitro-carburizing, thermally sprayed coatings, water droplet erosion

1. Introduction

Erosion of hydro and thermal power plant (HPP and TPP) components is a worldwide problem. It is typically present in the form of PE and CE for the hydro turbine components, resulting in their severe damages (Ref 1-3). PE is severe for all the HPPs located in Himalayan (India), Alpine (Europe), Andean (South America) regions, and at Yellow river in China. During monsoon season, it becomes impossible to control the silt passing through a hydro turbine. If unattended, the PE of critical components such as spears, guide vanes, labyrinth seals, runner blades, and seat rings leads to loss of turbine efficiency as high as 8-10% after an operation during one monsoon season. The silt concentration increases from 250 to 10,000 ppm and particle size exceeds 1000 μm . It is likely that more than 2500 MW power is lost every year due to PE of Indian HPPs and worldwide it exceeds manifold, resulting in a billion dollars revenue loss every year. CE as defined by Knapp et al (Ref 4) is a condition, when a liquid reaches a state at

which vapor cavities are formed and grow due to dynamic pressure reduction to the vapor pressure of the liquid at constant temperature. These cavities, when travel in a high pressure zone, reverse their growth and collapse implisively in a very short time (nanoseconds), generating microjets which have very high velocities (Ref 4, 5). The microjets, close to solid surfaces, produce indentations of several micrometers and repeated impacts cause material removal. During summer, the water level of a hydro dam drops and operating hydro turbines, under full load, at lower water head and increased speed, leads to CE due to reduced cavitation number. Information on the water impingement erosion (WIE), which is similar to CE and WDE, is already available in Ref 6-10. Lesser et al (Ref 8, 9) and Field et al (Ref 10) have reported that a liquid jet having higher impact velocity produces cavitation clouds, causing material removal similar to CE. The criterion for correlation of CE, WDE, and WIE with the mechanical properties of a material remains same (Ref 7, 11, 12). 13Cr4Ni, X20Cr13, and 17Cr4Ni PH stainless steels are commonly used for the manufacture of hydro turbines and water re-circulating pumps because of their excellent mechanical properties. The PE-, CE-, and WIE-damaged hydro turbine runner blades of a low head (27 m) Kaplan turbine, a spear of a medium head (488 m) Pelton turbine, and a guide vane of a medium head (493 m) Francis turbine are given in Fig. 1.

The induced draft (ID) fan blades, air pre-heaters (APHs) sector plates and seals, steam turbine inlet guide vanes, and moving blades, boiler tubes, headers, and diaphragms of a TPP are prone to excessive PE damages (Ref 13-15). The PE of an APH/ID fan is because of waste combustion products which

B.S. Mann, BHEL Corporate R&D, Vikasnagar, Hyderabad 500093, India. Contact e-mail: mann_balbir@yahoo.com.

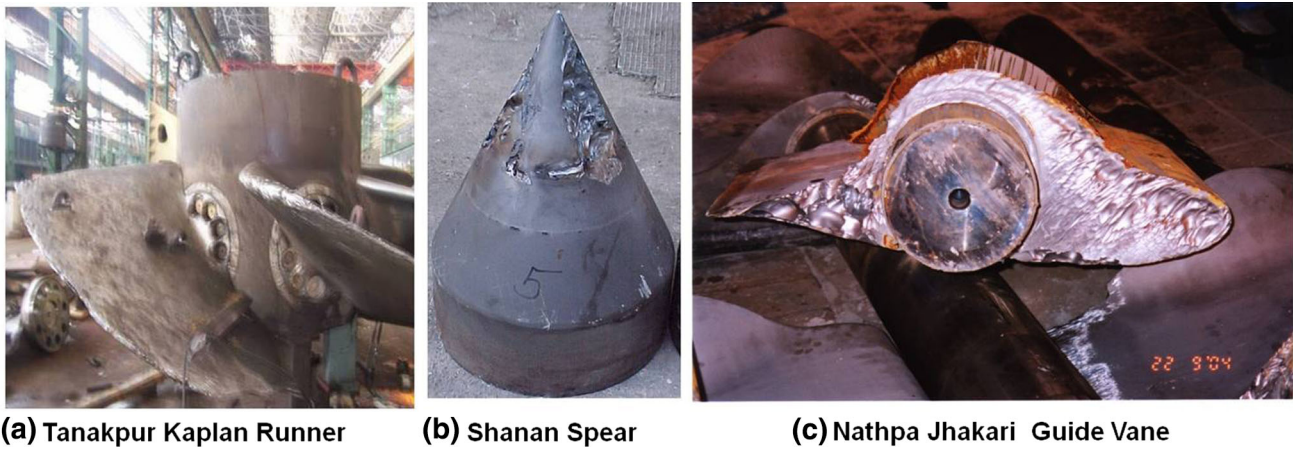


Fig. 1 Damaged hydro turbine components after one monsoon season; (a) Kaplan runner of a low head 3×40 MW Tanakpur HPP, (b) Pelton spear of a medium head 1×50 MW Shanan HPP, and (c) guide vane of a medium head 6×250 MW Nathpa Jhakri HPP

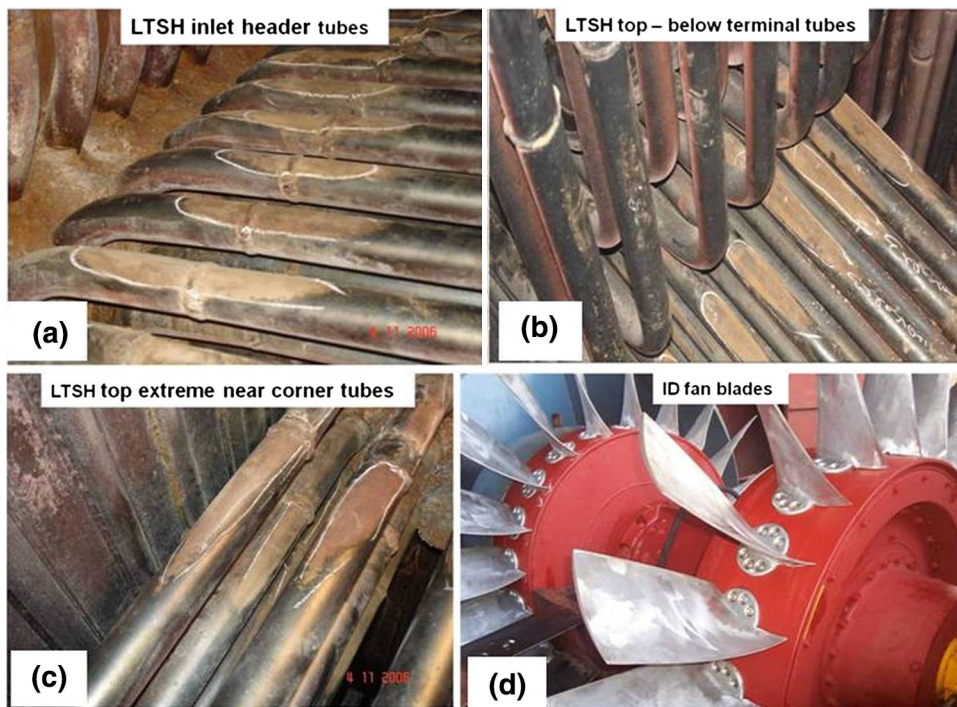


Fig. 2 Damaged LTSH boiler tubes from 250 MW Panipat TPP; (a) header tubes, (b) terminal tubes, (c) corner tubes, and (d) ID fan

contain abrasive fly ash particles (~ 50 to $63 \mu\text{m}$). A severely affected ID fan is shown in Fig. 2(d). The operating temperature of an APH is around 380°C and that of an ID fan is around 140°C . WC-CoCr-, WC-CrC-Ni-, Cr_3C_2 -NiCr-, and Cr_3C_2 -CoNiCrAlY-based high pressure high velocity oxy-fuel (HP-HVOF) coatings are preferred at these temperatures. The Cr_3C_2 -NiCr- and Cr_3C_2 -CoNiCrAlY-based HP-HVOF coatings are generally used for high temperature applications ($>400^\circ\text{C}$). The PE of diaphragms, bypass, and control valves, LP casing, inlet guide, and moving blades of a steam turbine are mainly because of magnetite scale inside the steam generator, boiler tubes, headers, and other steam flow paths exposed to high temperature during operation. This scale builds

up gradually and after a certain level it cracks and spalls, being brittle in nature, it breaks into angular particles of sizes 50 to $60 \mu\text{m}$ and erodes all these components. During initial hours of operation, around $80,000$ h, little or no erosion is observed; however, after an additional $40,000$ h of operation, severe erosion occurs. In fact, the inlet leading edges of a typical 800 MW low pressure steam turbine (LPST) moving blades have eroded 12 - 13 mm from their original dimensions in this time increment (Ref 14). The inlet guide blades are made of AISI 403 or AISI 410 stainless steel and LPST moving blades are made of either martensitic stainless steel (X20Cr13/X10CrNiMoV1222) or precipitate-hardened stainless steel (17Cr4Ni PH/X5CrNiCuNb16-4). Tables 1 and 4 give their

Table 1 Materials and coatings used for WDE, CE, and PE testing and their compositions

Materials	Composition, wt. %
X10CrNiMoV1222 (substrate)	0.1C, 0.25Si, 0.7Mn, 12Cr, 2.5Ni, 1.75 Mo, 0.3V, bal* Fe
X20Cr13 (substrate)	0.20C, 12Cr, 0.5Si, 0.5.0Mn, 0.5Ni, bal* Fe
13Cr4Ni (substrate)	0.058C, 12Cr, 3.85Ni, 0.5Si, 0.5Mo, bal* Fe
17Cr4Ni PH (substrate)	0.06C, 15.67Cr, 4.25Ni, 0.27Si, 0.64Mn, 3.6Cu, 0.19Nb, bal* Fe
10CrMo910 (substrate)	0.12C, 2.25Cr, 0.5Si, 0.6Mn, 1.2Mo, bal* Fe
Ti 6Al 4V (substrate)	6Al, 4V, bal* Ti
SHS7170 wire (TWAS coating)	Cr < 25, Mo < 10, W < 10, Mn < 5, B < 10, C < 5, Si < 5, bal* Fe
WC-CoCr powder (HP- HVOF coating)	10Co, 4Cr, bal* WC

X20Cr13 and X10CrNiMoV1222 stainless steels 'as forged' are used for LPST blades. At present, these are being replaced by Ti6Al4V alloy. 13Cr4Ni and 17Cr4Ni stainless steels are hydro turbine steels, used in 'as cast' and 'as forged' conditions. 10CrMo910 is a high-temperature creep-resistant steel, used in boilers and reactors
bal*—balance

Table 2 Microhardness, fracture toughness, FTMP, and PER of 'untreated' and 'HPDL treated' PINC layers, HP- HVOF, and TWAS coatings

Mechanical properties of HP-HVOF, TWAS, and PINC samples	'Untreated'	'HPDL treated'
HP-HVOF-coated X10CrNiMoV 1222, Microhardness, HV _{0.3} 0	1520	1845
HP-HVOF-coated X10CrNiMoV 1222, Fracture Toughness, K _{IC} , (MPa√m)	1.5	7.5
HP-HVOF-coated X10CrNiMoV 1222, HV _{0.3} × K _{IC} × 10 ³ , (FTMP), MPa√m × HV _{0.3}	2.28	13.84
HP-HVOF-coated X10CrNiMoV 1222, PE rate, (mm ³ /Kg of SiO ₂)	1.38	0.16
TWAS-coated X10CrNiMoV 1222 microhardness, HV _{0.3}	1118	910
TWAS-coated X10CrNiMoV 1222 fracture toughness, K _{IC} , MPa√m	3.77	7.15
TWAS-coated X10CrNiMoV 1222, HV _{0.3} × K _{IC} × 10 ³ , (FTMP), MPa√m × HV _{0.3}	4.2	6.5
TWAS-coated X10CrNiMoV 1222, PE rate, mm ³ /Kg of SiO ₂	8.44	3.80
PINC layers on X10CrNiMoV 1222, Microhardness, HV _{0.3}	1139	816
PINC layers on X10CrNiMoV 1222, PE rate, mm ³ /Kg of SiO ₂	4.37	5.43

The fracture toughness of X10CrNiMoV1222 'PINCAS' and X10CrNiMoV1222 'PINCLH' samples could not be measured because the indentation diagonals were found to have dimensions more than those of PINC layers' case depth (~80 μm) at loads required for reasonable crack formation (Fig. 5a). FTMP of the coatings = Fracture toughness (K_{IC}) × microhardness (HV_{0.3})

compositions and properties. Ti6Al4V alloy LPST blades are also used because of their higher strength-to-weight ratio. All these alloys are less resistant to PE and their application becomes more critical when WDE occurs due to condensation of steam (< 100 °C) in low pressure (LP) section, especially in the high-rating steam turbines above 500 MW and nuclear steam turbines of all ratings. The shaft and impellers of a boiler feed water pump are also affected even though these are made of high strength 17Cr4Ni PH and 13Cr4Ni stainless steels. The super heater coils, water wall tubes, and coal burner nozzles of a pulverized coal boiler (PCB) are also severely affected due to PE. Damaged low temperature super heater (LTSH) water wall tubes are given in Fig. 2(a)-(c). The atmospheric and circulating fluidized bed combustors (AFBC and CFBC), as compared to PCB, are more susceptible to PE especially the in-bed tubes and air nozzles. Presently, the PE-affected components are either coated with Tafa 140 MXC or SHS 7170 cored wire by TWA or Cr₃C₂- NiCr powder by HVOF/D-gun (Ref 13, 15-27). Any tube failure leads to costly shut down of a power plant. Considering the revenue loss and practical difficulties in repairing/replacing the tubes, customers are demanding increased life of the boiler tubes. HP-HVOF coatings are

successful, since they have advantages in density and bond strength (Ref 28-33). Tungsten carbide- and chromium carbide-based HP-HVOF coatings are in use to combat WDE of the LP bypass valves and LPST moving blades (Ref 13). It is reported that high-power diode laser (HPDL) surface treatment has improved their cavitation erosion resistance (CER) and water droplet erosion resistance (WDER) manifold, whereas the improvement in the particle erosion resistance (PER) is marginal (Ref 3, 6, 11). The coating properties such as fracture toughness, microhardness, and their product (FTMP) after laser surface treatment are given in Tables 2 and 4 and Ref 3, 11, 12, 15.

The article reviews the work carried out in the area of HPDL surface treatment of martensitic and precipitate-hardened stainless steels (13Cr4Ni, X20Cr13, X10CrNiMoV1222, and 17Cr4NiPH), Ti6Al4V alloy, and their protective coatings such as plasma ion nitro-carburized (PINC) layers, HP-HVOF, and twin-wire arc sprayed (TWAS) coatings which have been used up to now in hydro and thermal power plants to minimize their PE, CE, and WDE damages. WDE test results of these materials and coatings, which were HPDL treated at 1550 °C and tested maximum up to 8.55 million cycles at

57.167×10^6 J/m²s energy flux, are already available in Ref 6, 7, 11, 34-36. These were further tested up to 10.43 million cycles. X20Cr13 and X10CrNiMoV1222, the most common martensitic stainless steels, used in hydro and thermal power plants, were HPDL treated at higher temperature (1650 °C) and their WDE testing was also carried out up to 10.43 million cycles. Their XRD phases were analyzed and compared with the XRD data of these steels, which were HPDL treated at 1550 °C. After conducting long-range WDE tests, the correlation of CE, WDE, and PE resistances of these materials and protective coatings with their mechanical properties such as fracture toughness and micro-hardness product (FTMP), ultimate resilience (UR), modified resilience (MR), and ultimate modified resilience (MUR) has been reviewed and discussed. One of the edges of a 500 MW LPST moving blade (X10CrNiMoV1222 stainless steel) was HPDL surface treated at 1550 °C and its radii of curvatures and deflections were measured and compared with those of a flat rectangular sample of size 100 × 50 × 6 mm, which was also HPDL treated at 1550 °C (Ref 6).

2. Earlier Findings

2.1 PINC Layers, TWAS and HP-HVOF Coatings, and Their HPDL Surface Treatment

2.1.1 HP-HVOF and TWAS Coatings. It is reported in Ref 3, 6, 7, 11, 32, 35-37 that the WC-10Co4Cr-based HP-HVOF and SHS 7170-based TWAS coatings are being applied on stainless steel (X10CrNiMoV1222 and X20Cr13) rectangular blocks as well as on the round samples (Ø 12.70 × 40 mm) using a robotically controlled advanced-liquid-fuel HP-HVOF and Hobart Tafa 9000 TWA spraying systems. The robotic facility consists of a six axes articulated foundry version robot along with a two axes tilt-turn table (BHEL Corporate R&D, India). X10CrNiMoV1222 stainless steel is commonly used in a 500 MV and higher rating steam turbines, and X20Cr13 stainless steel is used in lower rating steam turbines. The thermal spray gun (advanced-liquid-fuel based HP-HVOF or TWA) is mounted on the robot arms and job is mounted on a turntable. Their movements are programmed as per the requirements and controlled remotely from the robot controller during operation. The facility ensures an excellent non-porous and properly adherent coating along with uniform thickness of precise accuracy. The facility also consists of a real-time diagnostic and control system. The particles' parameters such as velocity, temperature, and molten state along with the substrate temperature are controlled in real time and are maintained within limits. These parameters are monitored by using a particle monitoring system (Accuraspray, Tecnar, Canada). This control enables highly engineered coatings, such as tailoring or grading of composition at interfaces. The HP-HVOF and TWAS coating preparation and spraying parameters are given in Ref 6, 7, 11, 32, 35-37. The coating thickness, in the range of 300 ± 30 µm, is maintained on all the test samples. A thin boride bond coat ~100 ± 30 µm thick is also given. This is to ensure a metallurgical bond with the substrate to minimize thermal mismatch between substrate and coating. The thermal mismatch arises due to sudden heating and cooling of the samples during HPDL surface treatment and without a bond coat, the thermally sprayed coatings (HP-HVOF and TWAS) generally get cracked.

2.1.2 PINC Layers. Plasma ion nitro-carburizing (PINC) furnaces are used regularly for building PINC layers on the finished stainless steel and titanium alloy components. PINC is a process by which the surface hardness of a material is improved due to diffusion of carbon and nitrogen atoms up to a few hundred micron depth (case) under the surface. The carbon and nitrogen, which enter in a material, form hard nitrides and carbides. PINC layers are generally pore free and have a metallurgical bond with the substrate because these are processed in an ionized oxygen-free environment. By maintaining proper plasma ion parameters, such as temperature: 480-550 °C, chamber pressure: 1.8 Torr, bias voltage: 480V DC and LPG/NH₃ gases flow rates: 1-1.5%, duration: 8 h. A case depth of around 80 µm has come automatically on X10CrNiMoV1222 stainless steel, free from white layer (Ref 34, 37). In conventional gas nitro-carburizing, the outer white layer is formed which is hard, brittle and lacks CER, PER and WDER. In PINC process, this white layer is avoided by selecting proper parameters.

2.1.3 HPDL Surface Treatment. The robotic HPDL facility, consisting of a 4.6 kW diode laser (Laserline, GmbH) having '20 mm x 2.8 mm' and '30 mm x 3 mm' laser, is used for the surface treatment of materials and coatings (Ref 3, 6, 7, 12, 38-40). CO₂ laser has also been used for the surface treatment of HVOF coating (Ref 39, 41). The manipulation of the laser beam, round test samples, and rectangular blocks is being carried out by a six plus two axes robot (Kuka, GmbH), in which all the eight axes are synchronized. Laser beam power is controlled in a closed loop by two-color pyrometer, and a uniform surface temperature of the round test samples and rectangular blocks in the range of 1550 ± 12.5 °C is maintained. The robot is programmed in such a way that the laser beam tracks the coated block and round test samples at an optimum speed (1.5-5 mm/s) ensuring uniform surface temperature. Proper compressed air cooling of the steel blocks and round samples is maintained throughout the HPDL treatment. The laser power on/off is also controlled by the robot. The CE test samples as per ASTM G32-03 and PE test samples of size 50 × 50 × 6 mm are being made from the HPDL-treated rectangular blocks. Laser power densities of the samples, which were WDE tested as per Test I and Test II of Table 3, are in the range of 770-1150 and 1725-1975 J/cm², respectively, whereas for CE and PE test samples, these are in the range of 2300-2530 J/cm². The laser power densities of the flat rectangular samples (100 × 50 × 6 mm) which were used for the deflection and residual stress measurements are in the range of 1150-1626 J/cm² (Ref 6). For a job, once its surface temperature and laser scan speed are selected, different HPDL power densities come automatically depending upon of its thermal response. The laser power density of titanium alloy is less than those of stainless steels because of its lower thermal diffusivity (Ref 12, 40). Similarly the thermal response of the rectangular blocks and round samples is not same even though their surface temperatures are same. Typical surface temperature/laser power time cycles (STLPTC) of Ti6Al4V alloy and 13Cr4Ni stainless steel flat samples, which are HPDL treated at 1550 ± 12.5 °C are shown in Fig. 3 and for other materials and coatings, these cycles are available in Ref 7, 40, 42.

2.2 Microhardness and Fracture Toughness

The Vickers microhardnesses of HPDL-treated and untreated stainless steel, Ti6Al4V alloy, PINC layers, TWAS, and

Table 3 WDE experimental test conditions

Conditions	Test I	Test II
Water impacted per cycle, mL	0.023	0.035
Water impact energy, J	0.250	0.380
Water energy flux, J/m ² s	37.158 × 10 ⁶	57.167 × 10 ⁶
Water mass flux, m/s	3.44	4.0 m/s
Relative water velocity, m/s	147.6	147.6
Test sample size, mm	Ø 12.70 × 40	Ø 12.70 × 40
Number of specimens used	12	12
Test duration, cycles	13.176 × 10 ⁶	10.43 × 10 ⁶
Angle of impact	0°-90°	0°-90°
Impact frequency, Hz	79.166	79.166
Experimental accuracy	±15.5%	±15.5%
Salt concentration	As per Ref 6	As per Ref 7

Laser power densities, for the samples, which were WDE tested as per Test I, are in the range of 770-1150 J/cm² and those tested as per Test II are in the range of 1725-1975 J/cm²

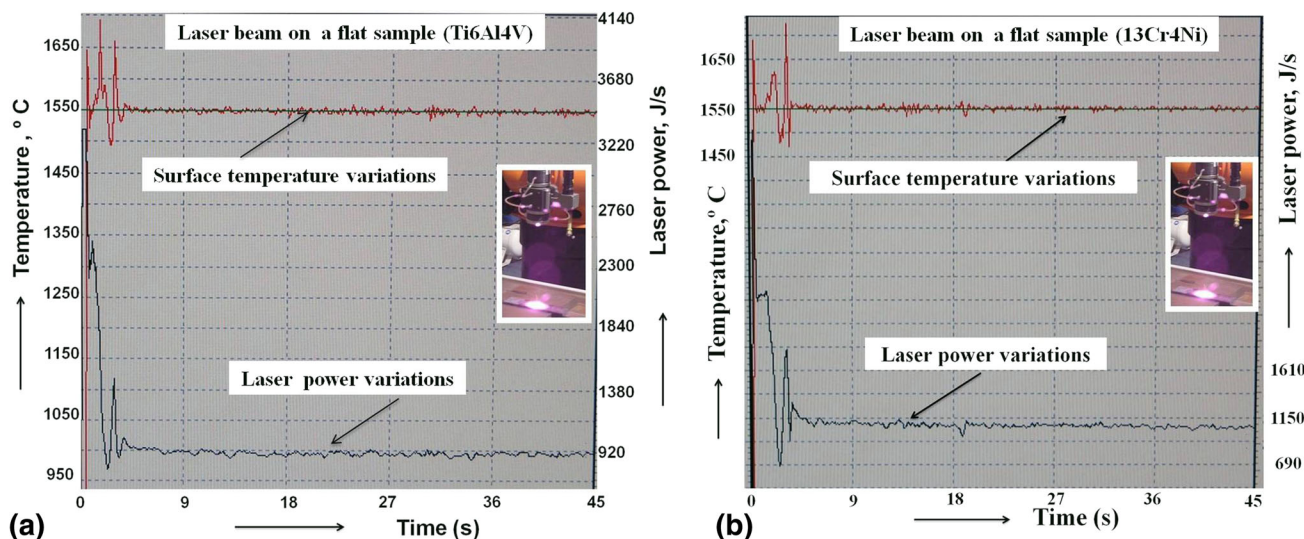


Fig. 3 STLPTC of (a) Ti6Al4V alloy and (b) 13Cr4Ni stainless steel flat samples showing less laser power density for Ti6Al4V alloy, Ref 12, 40

HP-HVOF-coated samples are generally measured using a microhardness hardness tester by applying loads up to 3 N with a dwell time of 13 s. The fracture toughness (K_{IC}) of the PINC layers, TWAS, and HP-HVOF coatings is measured by applying higher loads; cracks are initiated at the edges of the indents on their mirror-polished cross sections and K_{IC} values are calculated as per Ref 43. Typical Indents created on the cross sections of HP-HVOF coating and PINC layers are shown in Fig. 4 and 5, respectively (Ref 3, 37). Loads up to 300 N are applied on the thermally sprayed samples, whereas loads up to 20 N are applied on PINC layers. The microhardness and fracture toughness measurement details are already available in Ref 3, 6, 11, 12, 32, 34-38, 40, 42. It is not possible to initiate cracks at the edges of an indent in the HPDL-treated and untreated stainless steels and titanium alloy samples because these are highly ductile, hence their fracture toughness cannot be measured by this technique. It is reported that the microhardness of “as-sprayed” WC-10Co4Cr HP-HVOF coating on X10CrNiMoV1222 stainless steel (X10CrNiMoV1222‘HVOFAS’ sample) comes around 1520 HV_{0.3}

(standard deviation 28.5 HV_{0.3}) and after HPDL treatment (X10CrNiMoV1222‘HVOFLH’ sample) the value is around 1845 HV_{0.3}. The microhardness of “as-sprayed” SHS 7170 TWAS coating (X10CrNiMoV1222‘TWASAS’ sample) is 1118 HV_{0.3} and after HPDL treatment (X10CrNiMoV1222‘T-WASLH’ sample) the value has dropped to 910 HV_{0.3} (standard deviation 12 HV_{0.3}) in the laser-melted region. The microhardness of PINC layers on X10CrNiMoV1222 stainless steel (X10CrNiMoV1222‘PINCAS’ sample) is around 1139 HV_{0.3} and it has reduced to 816 HV_{0.3} after HPDL treatment (X10CrNiMoV1222‘PINCLH’ sample). The maximum microhardness observed on X20Cr13‘LH’ sample is around 580 HV_{0.3}, and that observed on X10CrNiMoV1222‘LH’ sample is around 550 HV_{0.3}. The microhardness observed on 13Cr4Ni‘LH’ and Ti6Al4V‘LH’ samples are around 400 HV_{0.3} and 370 HV_{0.3}, respectively. For 17Cr4Ni PH‘LH’ sample, the microhardness remained unchanged (~370 HV_{0.3}). The microhardness values of the samples and their identification (‘LH’- HPDL treated at 1550 °C and ‘AS’- untreated one) are given in Table 4. The microhardness versus

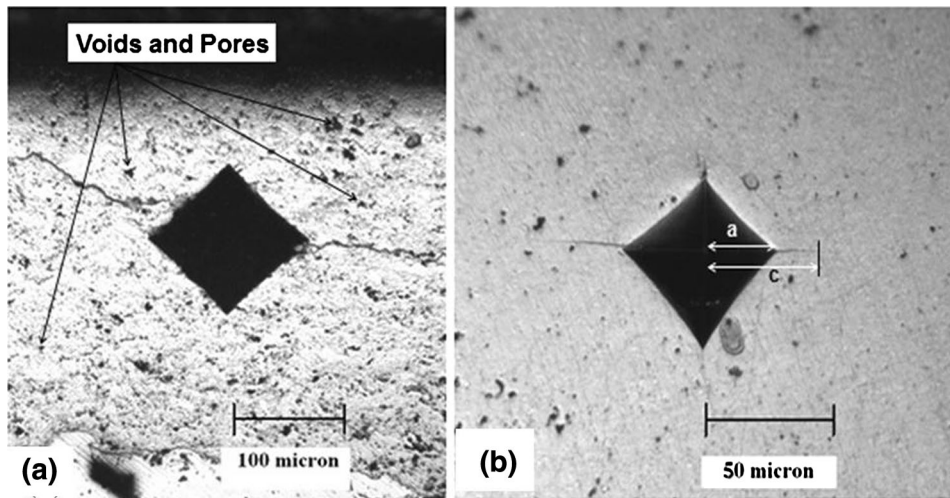


Fig. 4 Indentation on the cross section of (a) 'as sprayed' and (b) HPDL-treated HVOF coating at 50 N load. For HPDL-treated HVOF coating, ' a ' = 37.5 μm and ' c ' = 62.5 μm and for 'as sprayed' HVOF coating, ' a ' = 46.0 μm and ' c ' = 160.5 μm , Ref 3

Table 4 Mechanical properties of HPDL-treated coatings/materials and their volume losses due to CE, WDE, and PE

Materials	UTS, MPa	Hardness, HV _{0.3}	MR, HV	MUR, J/cm ³	Volume loss due to CE, WDE, and PE			
					CE/h, mm ³ /h	WDE*, mm ³	WDE**, mm ³	PE, mm ³ /kg
X10CrNiMoV1222'AS'	1000	295.0	0.714	2.42	1.32	ExD	26.5	5.00
X10CrNiMoV1222'LH'	...	550.0	1.33	8.4	0.24	4.42	2.13	4.75
X10CrNiMoV1222'TWASAS'	...	1118	2.70	34.7	...	peeled off	...	8.44
X10CrNiMoV1222'TWASLH'	...	910	2.2	23.0	0.084	1.62	...	3.80
X10CrNiMoV1222'HVOFAS'	...	1520	3.68	64.21	1.255	peeled off	1.9***	1.38
X10CrNiMoV1222'HVOFLH'	...	1845	4.46	94.60	0.16
X10CrNiMoV1222'PINCAS'	...	1139	2.75	36.0	0.248	16.42	...	4.37
X10CrNiMoV1222'PINCLH'	...	816	1.97	18.48	...	1.1	...	5.43
X20Cr13'AS'	876	270	0.56	1.83	...	ExD	ExD	4.92
X20Cr13'LH'	...	580	1.2	8.44	...	5.56	0.00	4.55
Ti6Al4V'AS'	874	340	1.24	3.17	0.64	ExD	5.29	6.56
Ti6Al4V'LH'	...	370	1.35	3.752	0.37	35.66	2.56	4.72
13Cr4Ni'AS'	892.2	280	0.62	1.96	1.85	ExD	ExD	6.64
13Cr4Ni'LH'	...	400	0.89	4.0	1.1	ExD	7.32	5.70
17Cr4Ni PH'AS'	1224	370	1.13	3.577	...	ExD	7.67	4.96
17Cr4Ni PH'LH'	...	370	1.13	3.577	...	ExD	6.97	4.85

'LH'—HPDL treated at 1550⁰ C and 'AS'—untreated one

HP-HVOF, high pressure high velocity oxy-fuel; TWAS, twin-wire arc sprayed; PINC, plasma ion nitro-carburized

ExD—Excessively damaged

WDE**—WDE tested as per test conditions given in Table 3 (I). The 10CrMo910'AS', X20Cr13'AS', and 13Cr4Ni'AS' samples got excessively damaged before completing 13.176 million cycles and these were removed (Fig. 8). Their volume losses cannot be compared

WDE*—WDE tested as per test conditions given in Table 3 (II)

HP-HVOF*** data are already available in (Ref 24). It has given a volume loss < 1.9 mm³ in WDE at 29.88 × 10⁶ J/m²s after 10.98 million cycles and has proved to be the best among all the materials such as titanium alloy and heat-treated X10CrNiMoV1222 stainless steels. At higher energy flux as per Table 3 (II), the "as sprayed" HP-HVOF coating peeled off and X10CrNiMoV1222'AS', X20Cr13'AS', 13Cr4Ni'AS', Ti6Al4V'AS', and 13Cr4Ni'LH' samples got excessively damaged before completing 6.039 million cycles (Fig. 9). These samples were removed, hence, their volume losses, for a long duration, cannot be compared. The volume losses, due to CE for 8 h, and PE after impacting 1.5 kg of SiO₂ are given in the above Table

case depth plot of PINC layers on 13Cr4Ni stainless steel (13Cr4Ni'PINCAS' sample) is given in Fig. 6(b). Figure 6(a) gives microhardness versus case depth plots of 13Cr4Ni'LH' and X10CrNiMoV1222'LH' samples (Ref 37). The microhardness of HPDL-treated stainless steel, titanium alloy, PINC

layers, TWAS, and HP-HVOF-coated samples is given in Table 4. The fracture toughness calculations are carried out by using the Evans and Charles equation (Ref 43); $K_{IC} = 0.079 p / a^{3/2} \times \log(4.5 a/c)$, MPa√m, where ' p ' is applied load, ' a ' is the half indent diagonal, and ' c ' is the crack length from center of

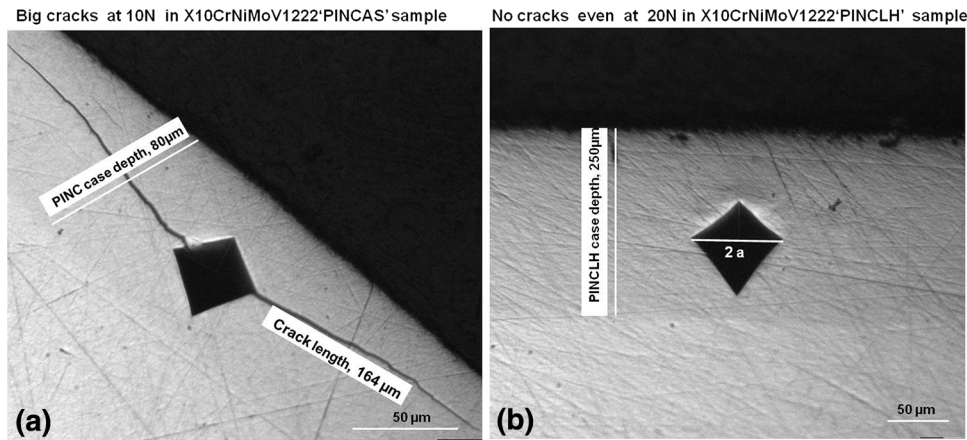


Fig. 5 Optical micrographs of (a) X10CrNiMoV1222'PINCAS' sample, showing big cracks at 10 N and (b) X10CrNiMoV1222'PINCLH' sample, showing no cracks even after applying a load of 20 N

the indent (Fig. 4). The fracture toughness on the cross section of X10Cr-NiMoV122'HVOFAS' sample is around 1.5 MPa \sqrt{m} , whereas that observed on the X10CrNiMoV1222'HVOFLH' sample is 7.5 MPa \sqrt{m} . The fracture toughness of X10CrNiMoV1222'PINCAS' and X10CrNiMoV1222'PINCLH' samples could not be measured because the indentation diagonals were found to have dimensions more than that of their case depth at loads required for reasonable crack formation. Fig. 5(a) and (b) shows the diamond pyramid impressions created on the cross section of untreated and HPDL-treated PINC layers, respectively. The load applied on the untreated sample is around 10 N, whereas that applied on HPDL-treated sample is around 20 N. The higher loads are generally applied on TWAS coating (100-300 N) and lower loads are applied on the HP-HVOF coating (50 N). For HPDL-treated SHS 7170 TWAS coating, the K_{IC} is 7.15 MPa \sqrt{m} at 300 N load, whereas for untreated one, this value is 3.77 MPa \sqrt{m} at a load of 50 N. Measurements at 300 N on the untreated SHS 7170-based TWAS coating could not be carried out since the coating got shattered at lesser loads (\sim 100 N). The measurement of the crack lengths at lower load ($<$ 50 N) on HPDL-treated WC-10Co4Cr-based HP-HVOF and SHS 7170-based TWAS coatings becomes difficult as the indent sizes are very small and cannot be measured and compared with those of PINC layers. The FTMP of X10CrNiMoV1222'HVOFLH' and X10CrNiMoV1222'TWASLH' samples is given in Table 2. It is seen from the Tables 2 and 4 that the K_{IC} of X10CrNiMoV1222'HVOFLH' sample is around 5 times, FTMP is around 6 times, and PER is around 8.6 times more than that of X10CrNiMoV1222'HVOFAS' sample. The K_{IC} , FTMP, and PER of X10CrNiMoV1222'TWASLH' sample are around 150 to 200% more than those of X10CrNiMoV1222'TWASAS' sample.

2.3 Scanning Electron Micrographs

SEM micrographs of HPDL-treated and untreated X20Cr13, 13Cr4Ni, X10CrNiMoV1222, 17Cr4Ni PH stainless steels, Ti6Al4V alloy, thermally sprayed coatings, and PINC layers are available in Ref 3, 6, 7, 11, 35-38, 40, 42. It is reported that the grain size is much smaller for all the HPDL-treated samples including coatings. For the HPDL-treated precipitate-hardened stainless steel (17Cr4Ni PH'LH' sample), there is a substantial refinement of its microstructure; however, the improvements in

its WDER and PER are marginal, 9 and 2%, respectively, (Table 4, Fig. 8 and Ref 42). This is because its MUR has not improved after HPDL treatment (Table 4). In case of martensitic stainless steels and titanium alloy, the grain size and MUR have improved significantly and WDER has also improved accordingly. Typical micrographs of Ti6Al4V alloy after HPDL treatment, showing fine microstructures, are given in Fig. 7 (Ref 7) and its improved WDE resistances at two different energy fluxes are given in Fig. 8 and 9.

2.4 PE, WDE, CE, and Residual Stresses

2.4.1 PE Discussions. The PE test facility, as per Ref 3, 11, 35, consists of a convergent nozzle through which mineral sand of size 180-250 μ m having hardness around 1100 HV, thoroughly mixed with water, impinges on the test sample. The slurry passes through 4 mm dia. \times 40 mm long tungsten carbide throat, providing a uniform jet velocity of 29.0 m/s. The rectangular sample of size 50 \times 50 \times 6 mm is kept in front of the sand-laden water jet at 45°. The PE test results of HPDL-treated and untreated 13Cr4Ni, 17Cr4Ni PH, X10CrNiMoV1222, X20Cr13 stainless steels, Ti6Al4V alloy, PINC layers, WC-10Co4Cr HP-HVOF, and SHS 7170 TWAS-coated samples are given in Table 4. It can be seen from Table 4 that the PER of X10CrNiMoV1222'HVOFLH' sample is around 29.7 times more than that of X20Cr13'LH'/X10CrNiMoV1222'LH'/ Ti6Al4V'LH' samples and around 8.6 times more than that of X10CrNiMoV1222'HVOFAS' sample. WC-10Co4Cr HP-HVOF coating after HPDL treatment, as explained earlier, is dense, free from voids, pores, and microcracks, whereas untreated one has a few voids, pores, and microcracks (Fig 4a and b, Ref 3). It is seen from Table 4 that X10CrNiMoV1222'HVOFLH' sample has the highest MUR and PER. The "as sprayed" SHS 7170 TWAS coating has excessive defects and is highly porous and it has become very dense after HPDL surface treatment (Ref 35). The "as deposited" PINC layers are brittle which is evident from appearance of very large cracks at lesser loads \sim 10 N (Fig. 5a). It has become very tough after HPDL surface treatment, showing no cracks even applying a load of 20 N (Fig. 5b, Ref 37). After HPDL surface treatment, the PER of SHS 7170 TWAS coating has improved more than twice as compared to untreated one. In case of HPDL-treated PINC samples, the PER

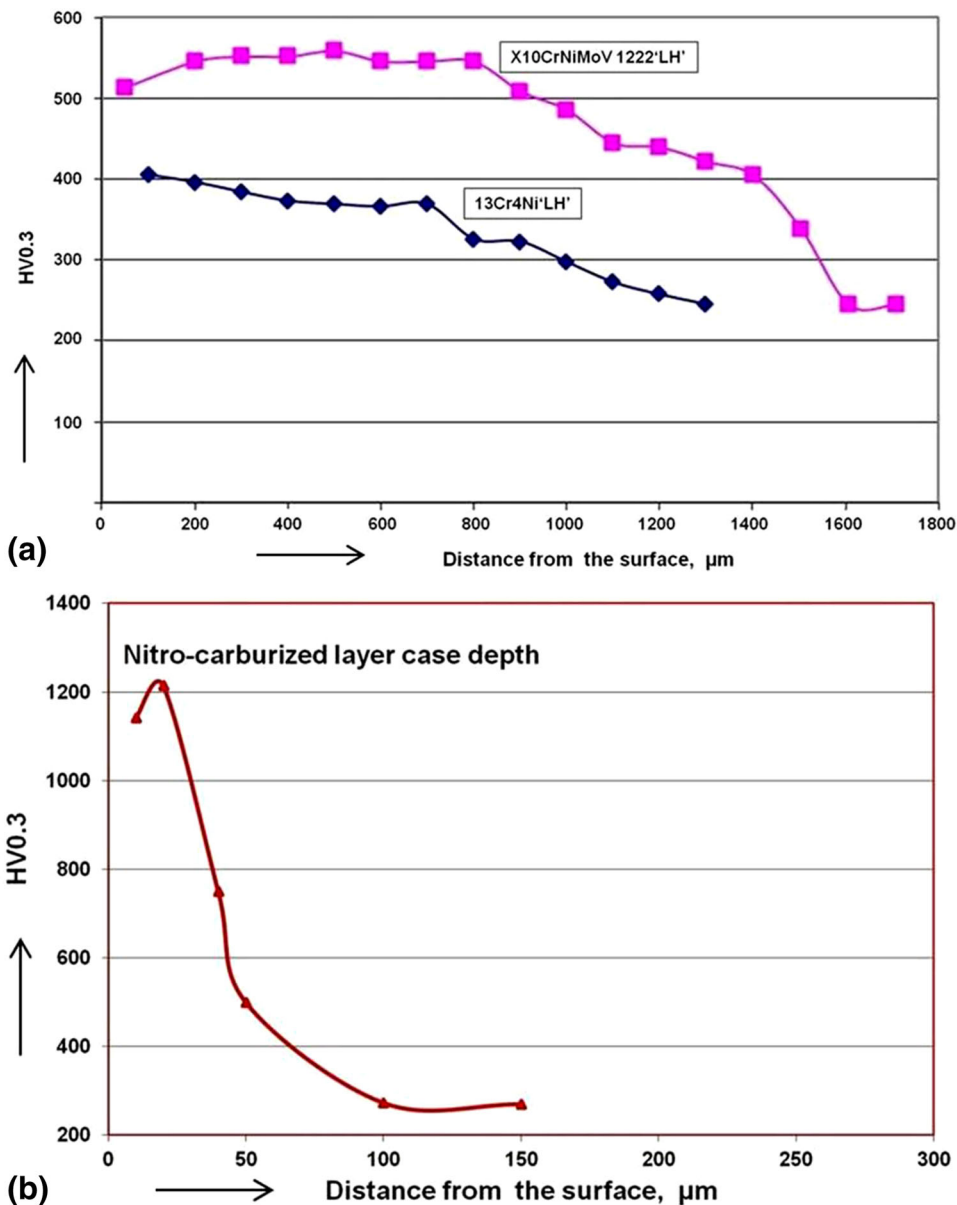


Fig. 6 Microhardness vs. case depth plots (a) of 13Cr4Ni'LH' and X10CrNiMoV1222'LH' samples and (b) of 13Cr4Ni'PINCAS' sample. The HPDL treatments were carried out at laser power densities ranging from 2300 to 2500 J/cm², Ref 37

has decreased. This may be because of substantial reduction in its microhardness from 1139 HV_{0.3} to 816 HV_{0.3} after HPDL surface treatment and it may not be enough to combat the impact of hard SiO₂ particles whose hardness is more than 1100 HV. The untreated PINC layers, "as sprayed" WC-10Co4Cr HP-HVOF, and SHS 7170 TWAS coatings are not considered for correlating their erosion resistances (PER, CER, and WDER) with MUR because these are not free from inherent defects. There is a marginal improvement in PER of HPDL-treated martensitic and precipitate-hardened stainless steels and titanium alloy as compared to untreated ones (Table 4). This improvement is insignificant as compared to the increased microhardness of the martensitic stainless steels. The WDER and PER of the coatings are available in Ref 3, 6, 11, 22-24, 32, 35.

2.4.2 WDE and CE Discussions. The details of WDE test facility, as per ASTM G73-1978, are already available in Ref 6, 7, 24, 32, 36, 38 and WDE tests parameters are given in Table 3. In short, the test facility consists of a round stainless steel disk, where the test samples are positioned in a housing of Ø 700 mm. Samples of size Ø 12.70 mm × 40 mm are affixed on the periphery of the disk. The disk is rotated at 79.166 Hz to obtain the test sample tangential velocity of 147.0 m/s. Two water jets impinge on the cylindrical test samples causing heavy damages. CE test set up consists of a high frequency high voltage signal generator which energizes the piezo-electric element in the converter via the transducer RF cable to oscillate at 20 kHz with amplitude of 50 microns (Ref 7, 12, 37). This mechanical vibration is transmitted to the horn, made of titanium alloy of matching impedance. The sample to be tested

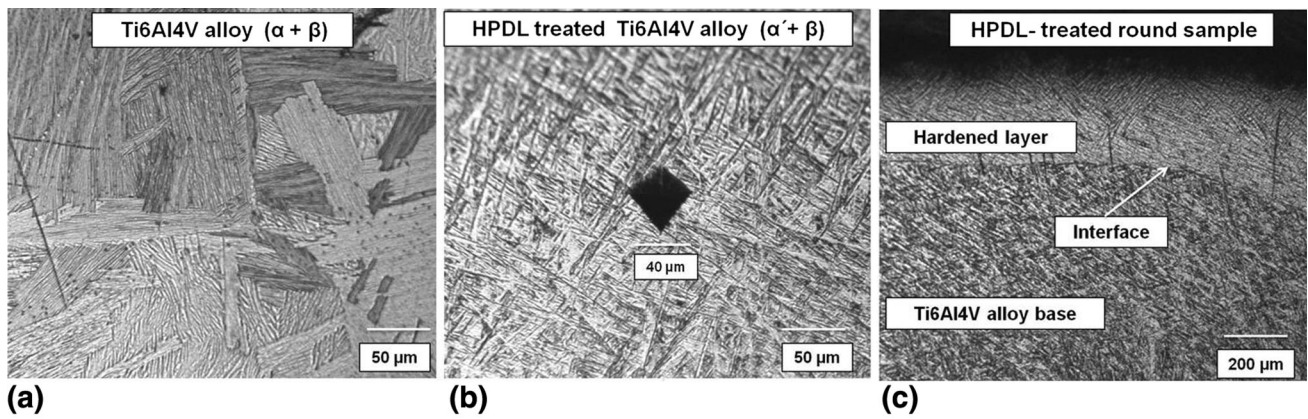


Fig. 7 Optical micrographs taken on the outer edge of a HPDL-treated Ti6Al4V alloy round sample, showing case depth, grain refinement, and formation of martensitic phase (α'). (a) untreated sample showing coarse grains ($\alpha + \beta$), (b) HPDL-treated sample showing fine grains ($\alpha' + \beta$), and (c) round sample showing case depth (Ref 7)

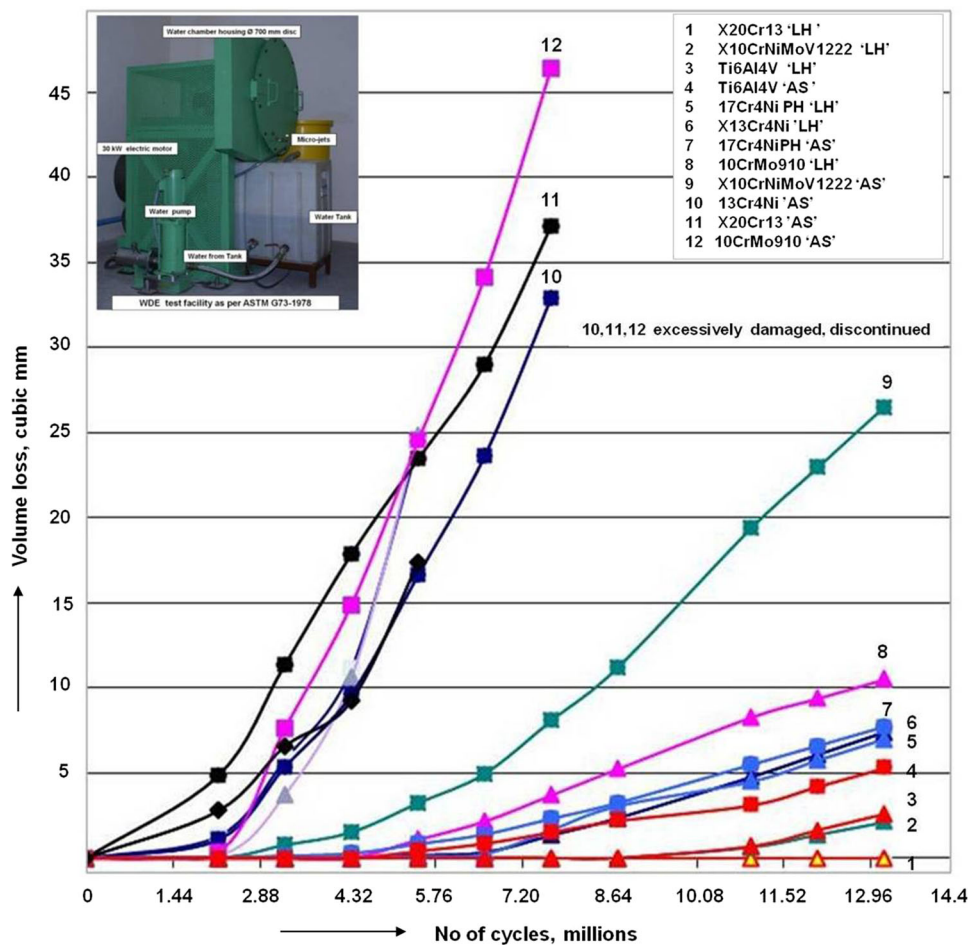


Fig. 8 Volume loss of HPDL-treated and untreated samples vs. WDE tests duration. The WDE tests were carried out as per ASTM G73-1978 by maintaining test parameters of Table 3 (Test I), Ref 6

is screwed into the horn tip and tightened to ensure that there is no loss of energy transfer from the horn tip to the sample. The sample also oscillates at a frequency of 20 kHz, thereby simulating cavitation phenomenon on its surface. The HPDL-treated and untreated martensitic and precipitate-hardened stainless steels, Ti6Al4V alloy, PINC, TWAS, and HP-HVOF-

coated samples are regularly tested for WDE and CE using these facilities. WDE test results of stainless steels and titanium alloy which were HPDL treated and at 1550 ± 12.5 °C, and tested up to 13.176 million cycles at 37.158×10^6 J/m²s energy flux are shown in Fig. 8 (Ref 6). It is seen from Fig. 8 that 10CrMo910'AS', X20Cr13'AS', and 13Cr4Ni'AS' samples got

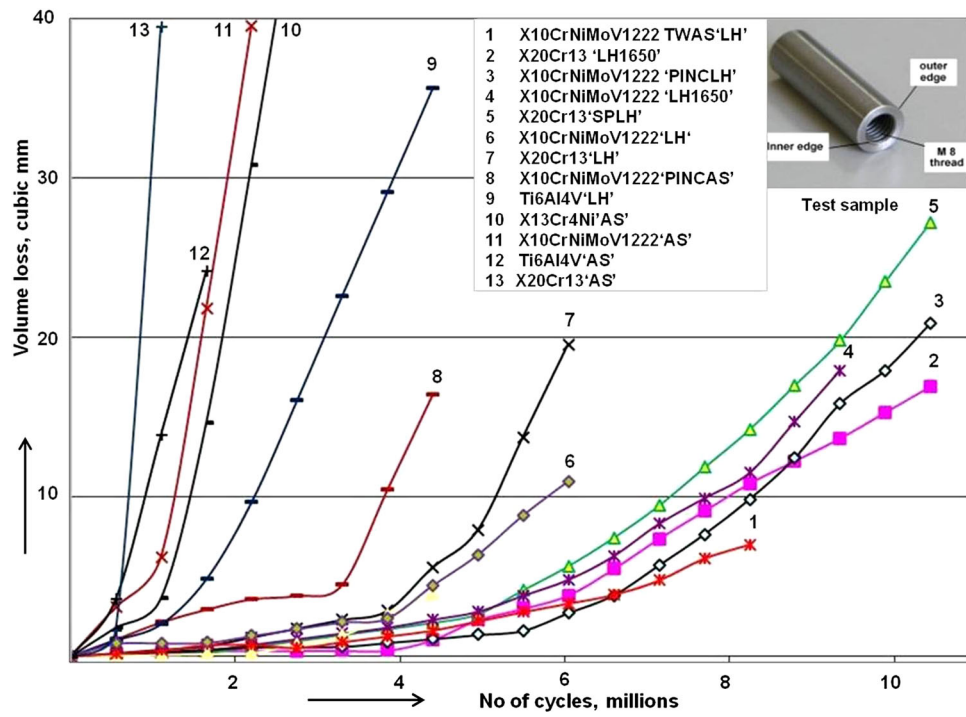


Fig. 9 Volume loss of HPDL-treated and untreated samples vs. WDE tests duration. The WDE tests were carried out as per ASTM G73-1978 by maintaining test parameters of Table 3 (Test II)

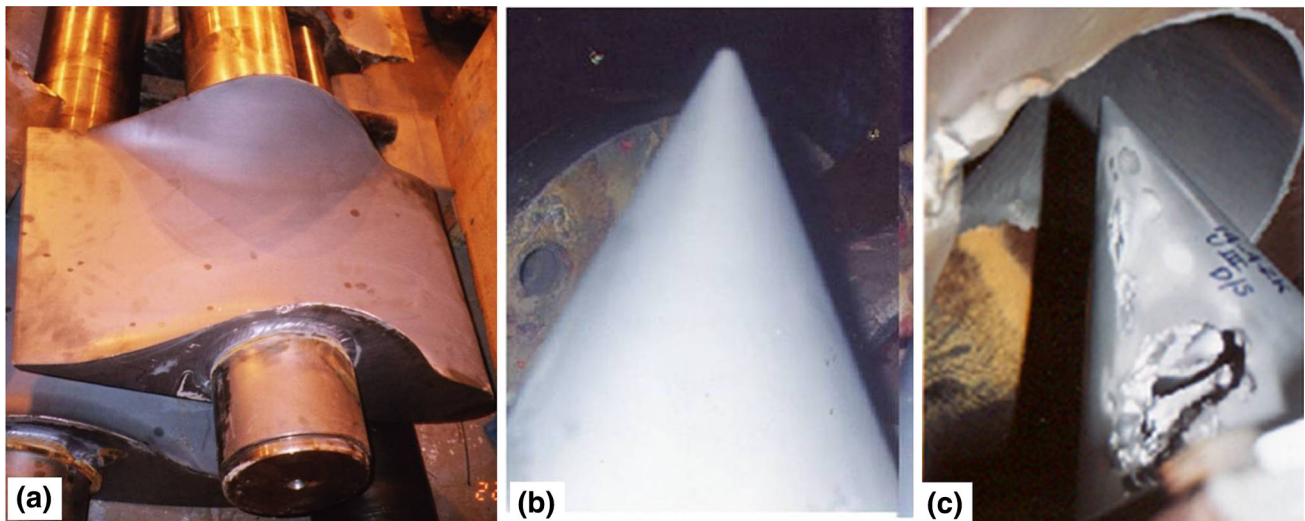


Fig. 10 Field performance of “as sprayed” HP-HVOF-coated components after one monsoon season; (a) guide vane of a medium head (493 m), 6×250 MW Nathpa Jhakri HPP, showing no damage (b) Pelton spear of a medium head (488 m), 1×50 MW Shanan HPP, showing no damage (c) Pelton spear of a high head (900 m), 3×40 MW Bhabha HPP, showing localized damage, as deep as 20 to 30 mm, Ref 3

excessively damaged before completion of 7.686 million cycles and their WDE testing could not be continued. At higher energy flux, 57.167×10^6 J/m²s, these tests discontinued even before completion of 6.039 million cycles (Fig. 9). It is also observed that X10CrNiMoV1222'TWASLH', X10CrNiMoV1222'PINCLH', and X20CR13'SPLH' samples have performed much better than other samples. X20Cr13'SPLH' sample is shot peened and HPDL treated at 1550 °C. Shot peening details are already available in Ref 38. The

“as sprayed” SHS 7170 TWAS and WC-10Co4Cr HP-HVOF coatings have peeled off during initial hours of the WDE and CE testing. After carrying out CE tests up to 8 h, the damages observed in X10CrNiMoV1222'AS', and Ti6Al4V'AS', 13Cr4Ni'AS' samples are high and their CE testing discontinued.

2.4.3 Deflections and Residual Stresses in Stainless Steel and Titanium Alloy Samples. Deflections, occurring due to HPDL surface treatment, are the main causes of residual

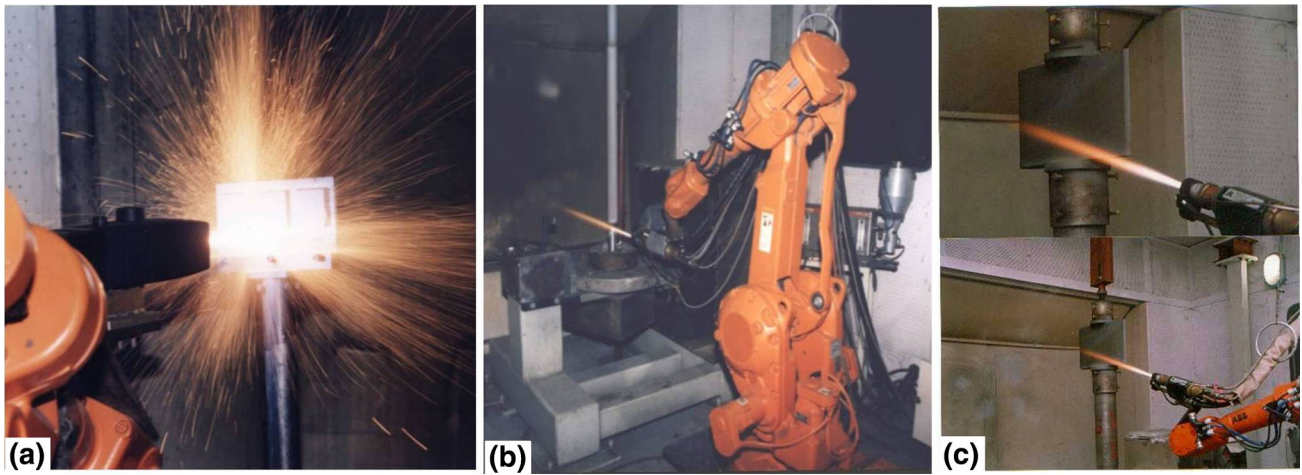


Fig. 11 Robotic controlled TWAS and HP-HVOF coatings being applied on (a) test coupons and (b) a boiler tube of a 250 MW PCB, (c) a guide vane of a hydro turbine

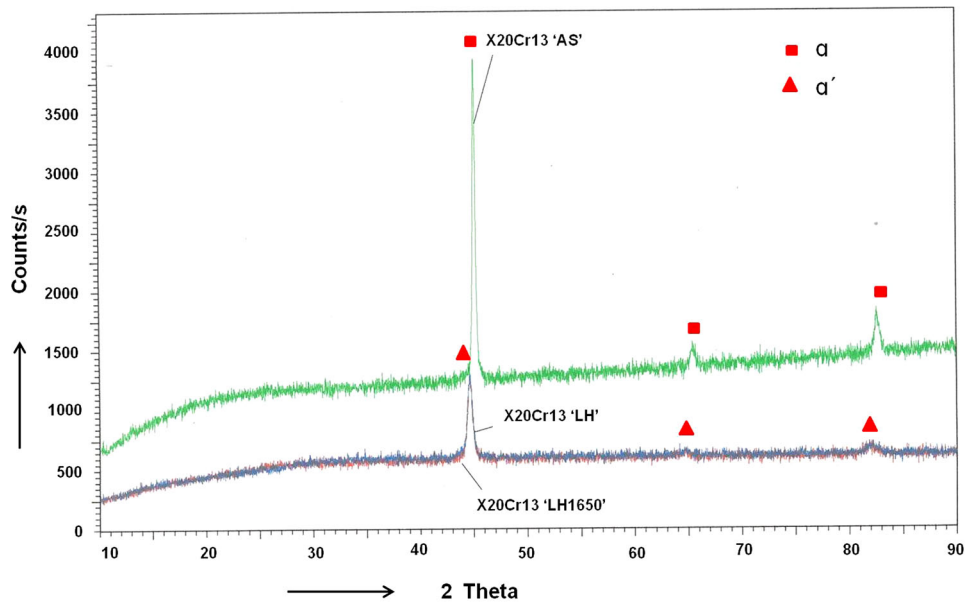


Fig. 12 XRD plots of X20Cr13'AS', X20Cr13'LH', and X20Cr13'LH1650' samples, showing α , and α' phases

stresses and their radii of curvatures can provide their magnitude. The maximum deflection recorded in the titanium alloy flat rectangular samples of size $100 \times 50 \times 6$ mm, is around $430 \mu\text{m}$, whereas that observed in the X10CrNi-MoV1222 stainless steel samples is around $200 \mu\text{m}$ (Ref 6). The HPDL parameters such as sample surface temperature ($1550 \pm 12.5 \text{ }^\circ\text{C}$), HPDL scan speed (1.5-5 mm/s) are being maintained similar to those maintained on the WDE test samples. The radii of curvatures of X10CrNiMoV1222 stainless steel samples are concave across the laser beam scan direction, resulting in compressive residual stresses (-247.3 MPa) and convex along the laser beam direction, resulting in tensile residual stresses ($+98.3 \text{ MPa}$ tensile). On the other hand, those observed in titanium alloy samples are concave in both the directions, resulting in compressive residual stresses (Ref 6). The deflections, hence the stresses,

arising in a particular material depend upon the geometry of the sample and its thermal response. Similar deflection and curvature trends were observed in flat rectangular iron samples earlier, though CO_2 laser was used (Ref 39). Moreover, the convections followed for measurement of radii of curvatures were different.

2.5 Field Performance

The field performance data of the robotically controlled HP-HVOF coatings from a number of Indian HPPs such as the Nathpa Jakhri, Shanan, Bhabha, and Baira Suil are already available in Ref 3. It is reported that the WC-10Co4Cr HP-HVOF-coated guide vanes and spears of the medium head hydro turbines have given encouraging results, whereas those of high head Pelton turbines have eroded locally as deep as 20

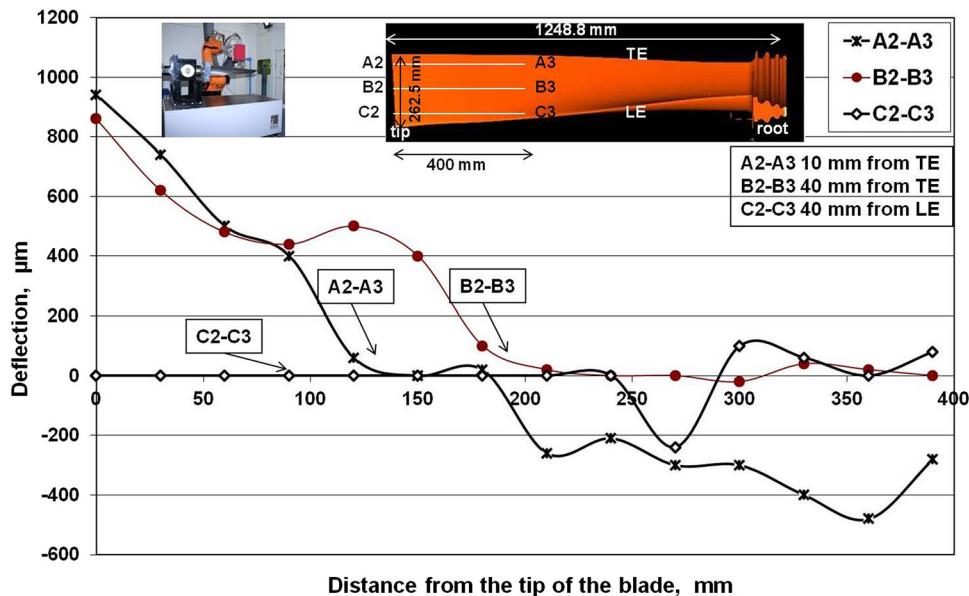


Fig. 13 Deflections due to HPDL treatment in a 500 MW LPST blade; the radii of curvatures at different sections of the blade are concave and convex, and are variable

to 30 mm during one monsoon season. This may be due to wearing out of the WC-10Co4Cr HP-HVOF coating locally and exposing the base material, that would have worn out very rapidly (Fig. 10). Overall, the extent of damage on the WC-10Co4Cr HP-HVOF coated spear is less as compared to uncoated ones. The robotically controlled WC-10Co4Cr HP-HVOF-coated guide vanes from a medium head hydro turbine performed very well during first year of operation; however, after two years of operation, these guide vanes got damaged heavily. Similar performance trends are observed at other HPPs. It is very well established that the robotically controlled HP-HVOF coating can enhance the life of PE damage-prone components of the medium head hydro turbine for a limited period (maximum one year). After two years of operation, damages similar to the uncoated ones are observed. The field performance data of robotically controlled Cr₃C₂ + NiCr HP-HVOF-coated high pressure diaphragms, steam valves, and nozzles of a steam turbine are already available in Ref 13. It is reported that the Cr₃C₂ + NiCr-based HP-HVOF coating has enhanced their life substantially. To combat WDE and to some extent PE, robotically controlled laser hardening of LPST moving blades is being carried out regularly and recently, it has been replaced by “as-sprayed” WC-10Co4Cr HP-HVOF coating because of its improved PER as compared to that of laser-hardened X10CrNiMoV1222 stainless steel (~3.44 times Table 4). The PER of “as-sprayed” WC-10Co4Cr HP-HVOF coating can be further improved by adopting HPDL surface treatment (~8.6 times) and can provide a lifelong solution. The HPDL-treated WC-10Co4Cr-based HP-HVOF coating is approximately 29.7 times better than HPDL-treated X20Cr13/X10CrNiMoV1222/Ti6Al4V alloy (Table 4). The water wall tubes, super heater coils, and coal burner nozzles of a PCB are being coated either with Cr₃C₂ + NiCr powder using HP-HVOF spraying system or with SHS 7170 cored wire using TWA spraying system (Fig. 11). HPDL-treated HP-HVOF and TWAS coatings may provide a lifelong solution.

3. Recent Findings

3.1 WDER of HPDL-Treated Stainless Steels and significance of XRD Phases

WDE test results of PINC layers (X10CrNiMoV1222‘PIN-CAS’ sample), HPDL-treated stainless steels, and titanium alloy (X20Cr13‘LH’, 13Cr4Ni‘LH’, X10CrNiMoV1222‘LH’, 17Cr4Ni PH‘LH’, and Ti6Al4V‘LH’ samples) up to 6.039 million cycles and those of HPDL-treated PINC layers (X10CrNiMoV1222‘PINCLH’ sample) and HPDL-treated SHS 7170 TWAS coating (X10CrNiMoV1222‘TwasLH’ sample) up to 8.55 million cycles at 57.167×10^6 J/m²s energy flux are already available (Ref 7, 34, 38). The HPDL surface treatment of all these materials and coatings was carried at 1550 ± 12.5 °C. The WDE testing of HPDL-treated PINC layers and TWAS coating was further continued up to 10.43 million cycles along with X20Cr13 and X10CrNiMoV1222 stainless steels samples, which were HPDL treated at 1650 °C (Fig. 9). Increased HPDL surface temperature from 1550 to 1650 °C of these two steels has improved their WDER significantly. The improvements in X10CrNiMoV1222‘LH1650’ and X20Cr13‘LH1650’ samples are around 200 and 500%, respectively, because of increased martensitic (α) phase at higher temperature (Fig. 12). Similar phase transformations and improved WDER were also observed in Ti6Al4V‘LH’ sample (Ref 7, 36). The “as sprayed” coatings (WC-10Co4Cr HP-HVOF and SHS770 TWAS) at higher energy flux (57.167×10^6 J/m²s) have peeled off. As explained earlier, that these coatings are not free from defects. In WC-10Co4Cr HP-HVOF coating (X10CrNiMoV1222‘HVOFAS’ sample), these defects are less, whereas in SHS 7170 TWAS coating (X10CrNiMoV1222‘TwasAS’ sample) these defects are more. The PINC layers do not have these defects and have a metallurgical bond with the substrate. The “as sprayed” WC-10Co4Cr HP-HVOF coating has been tested earlier in WDE at 29.88×10^6 J/m²s (Ref 24). At this energy flux, this coating has

proven to be the best among all the materials including heat-treated X10CrNiMoV1222 stainless steel (Table 4). So it is very difficult to compare all the materials and coatings in WDE at one energy flux because of excessive damages in untreated materials and coatings and negligible damages in HPDL-treated ones. This is the main reason of considering lower energy flux WDE test results for the comparison. The PER, CER, and WDER of “as sprayed” (SHS 7170 TWAS and WC-10Co4Cr HP-HVOF) coatings and “as deposited” PINC layers cannot be correlated with MUR because these are either defective or highly brittle. Appearance of big cracks in PINC layers (X10CrNiMoV1222‘PINCAS’ sample, Fig. 5 a) at very low load around 10 N is an evidence of the brittleness.

3.2 HPDL Surface Treatment of LPST Moving Blade and its Deflections

One of the edges (TE, being thinner) of a 500 MW LPST moving blade is HPDL surface treated, maintaining similar HPDL temperatures which were maintained on a flat rectangular X10CrNiMoV1222 stainless steel sample of size $100 \times 50 \times 6$ mm. For the LPST moving blade, these deflections, radii of curvature, and residual stresses are different from those of a flat rectangular sample, because it has a round leading edge. The measured deflections in LPST moving blade are $+940 \mu\text{m}$, at the tip of the blade toward trailing edge and $-480 \mu\text{m}$, at 360 mm from the tip toward root. Its radius of curvature, R_1 varies from 17234.5 mm at the tip of the blade to very large (infinite) toward root of the blade (Fig. 13). The variation is in a wavy form, contributing both types of the stresses (tensile as well as compressive). The radius of curvature, R_2 is 26310 mm (concave) across the laser beam scan direction, contributing compressive stresses, similar to that of a flat rectangular sample. The deflections (stresses), if excessive, are generally stress relieved by adopting a suitable stress relieving cycle so that these can be kept within specified design limits. The laser surface melting is completely avoided because it introduces excessive tensile residual stresses, leading to reduced fatigue life.

3.3 Correlation of Erosion Resistance with Mechanical Properties

The correlation of CER, PER, and WDER of HPDL-treated Ti6Al4V alloy, X20Cr13, X10CrNiMoV1222 stainless steels, SHS 7170 TWAS, and WC-10Co4Cr HP-HVOF coatings with mechanical properties such as UR, MR, MUR, and FTMP has been studied earlier (Ref 7, 24, 38). Materials based on UR have been correlated with CER and it is reported that UR is a valid mechanical property required for CER (Ref 4). For coated or HPDL surface-treated materials, UR does not hold good. As discussed earlier, the fracture toughness of HPDL-treated and untreated PINC layers (X10CrNiMoV1222‘PINCAS’ and X10CrNiMoV1222‘PINCLH’ samples) could not be measured, so their CER, WDER, and PER cannot be correlated with FTMP. On the other hand, initiation of cracks at the edges of an indent in HPDL-treated and untreated stainless steels and titanium alloy is not possible because these are highly ductile. Their K_{IC} cannot be calculated. It is not possible to correlate their CER, WDER, and PER with FTMP. These limitations of measuring mechanical properties of HPDL-treated stainless steels, titanium alloy, PINC layers, HP-HVOF, and TWAS coatings required for the calculation of MR and MUR are not there. Table 4 gives their values. It is also seen from Table 4

that the PER, WDER, and CER of HPDL-treated materials (martensitic and precipitate-hardened stainless steels, titanium alloy) and coatings (PINC layers, WC-10Co4Cr HP-HVOF, and SHS 7170 TWAS) have a better correlation with MUR rather than MR. The mechanical properties: UR, MR, MUR, and FTMP are defined as follows:

$UR = UTS^2/2E$, (area of the triangle obtained when the yield point is raised to UTS of the engineering stress-strain curve). $E =$ Young’s Modulus, UTS = ultimate tensile strength.

$MR = (UTS/2E)_{\text{substrate}} \times \text{Hardness}_{\text{top surface}}$, $MUR = UR_{\text{substrate}} \times (\text{Hardness}_{\text{top surface}}/\text{Hardness}_{\text{substrate}})^2$, $FTMP =$ Fracture toughness (K_{IC}) \times microhardness ($HV_{0.3}$).

CE, WDE, and PE values are given in Table 4. CER (h/mm^3), WDER (rev/mm^3), and PER (kg/mm^3) are inverse of these values.

4. Conclusions

While preparing a review, emphasis is given on the experimental investigations rather than basic principles of HPDL surface treatment. The studies are mainly focused on HPDL treatment of materials and coatings to combat CE, WDE, and PE damages of hydro and thermal power plant components. It is concluded from present and earlier findings that HPDL surface treatment eliminates most of the defects which exist in PINC layers, HP-HVOF, and TWAS coatings. It also improves the substrate properties, making it a promising potential candidate for hydro and thermal power plants. The microhardness of HPDL-treated WC-10Co4Cr HP-HVOF coating has increased, whereas those of HPDL-treated SHS 7170 TWAS coating and PINC layers have decreased. The fracture toughness of all these coatings after HPDL treatment has improved significantly where as those of PINC layers could not be measured because the indentation diagonals found to have dimensions more than the case depth at loads required for the initiation of reasonable cracks. The “as deposited” PINC layers being brittle and “as sprayed” WC-10Co4Cr HP-HVOF and SHS 7170 TWAS coatings, having inherent defects such as pores, voids, oxides, and microcracks, cannot be considered for correlating their CER, WDER, and PER with MR and MUR. The MUR of HP-HVOF coating, titanium alloy, and stainless steels, except 17Cr4Ni PH steel got improved after HPDL surface treatment. Among these, the X10CrNiMoV1222‘HVOFLH’ sample has the highest (11.22 times that of X10CrNiMoV1222‘LH’ sample). Its PER has also improved accordingly (29.7 times that of X10CrNiMoV1222‘LH’ sample). The PER of PINC layers (X10CrNiMoV1222‘PINCLH’ sample) has not improved, may be due to its reduced microhardness ($\sim 816 HV_{0.3}$) as compared to that of SiO_2 erodent ($> 1100 HV$).

After long duration of WDE testing (10.43 million cycles at $57.167 \times 10^6 \text{ J}/\text{m}^2\text{s}$), the X10CrNiMoV1222‘TwasLH’ X10CrNiMoV1222‘PINCLH’, X20Cr13‘SPLH’ X20Cr13‘LH1650’, and X10CrNiMoV1222‘LH1650’ samples have performed extremely well and performances of X20Cr13‘LH1650’ and X10CrNiMoV1222‘TwasLH’ samples are outstanding. The increased HPDL surface temperature of X10CrNiMoV1222 and X20Cr13 stainless steel samples from 1550 to 1650 °C has resulted in much improved WDER, more than 200 and 500%, respectively, because of increased martensitic phase (α). To combat PE of severely affected hydro

and thermal power plants components, HPDL-treated HP-HVOF coating may be the best choice. On the other hand to combat CE and WDE damages, HPDL-treated PINC layers or HPDL-treated thermally sprayed coating (TWAS and HP-HVOF) can be used. Higher temperature HPDL-treated martensitic stainless steels and titanium alloy may be used with care. There are chances of excessive tensile stresses in the components which may reduce their fatigue life. Shot peening followed by HPDL treatment may be a better option. Overall, HPDL-treated thermally sprayed coatings, having higher thickness and no limitations on the size of the components, are preferred.

Acknowledgments

The author is thankful to all the colleagues at the Centre of Excellence for Surface Engineering for their help during the course of the work and also to the management of BHEL Corporate R&D for giving an opportunity to work in this area.

References

1. B.S. Mann, High-Energy Particle Impact Wear Resistance of Hard Coatings and Their Application in Hydro Turbines, *Wear*, 2000, **237**, p 140–146
2. H. Grein and A. Schachenmann, Abrasion in Hydro-electric Machinery, *Sulzer Technical Review* 1/1992, vol 74, p 9–28
3. B.S. Mann, V. Arya, and B.K. Pant, High Power Diode Laser- Surface Treated HVOF Coating to Combat High Energy Particle Impact Wear, *J. Mater. Eng. Perform.*, 2013, **22**(7), p 1995–2004
4. R.T. Knapp, J.W. Daily, and F.G. Hammit, *Cavitation*, McGraw-Hill, New York, 1970
5. X. Escalera, E. Egusquiza, M. Farhat, F. Avellanb, and M. Coussirata, Detection of Cavitation in Hydraulic Machinery, *Mech. Syst. Signal Process.*, 2006, **20**, p 983–1007
6. B.S. Mann, V. Arya, B.K. Pant, and M. Agrawal, High-power Diode Laser- Surface Treatment to Minimize Droplet Erosion of Low-pressure Steam Turbine Moving Blades, *J. Mater. Eng. Perform.*, 2009, **18**(7), p 990–998
7. B.S. Mann, Water Droplet and Cavitation Erosion Behavior of Laser-Treated Stainless Steel and Titanium Alloy: Their Similarities, *J. Mater. Eng. and Perform.*, 2013, **22**(12), p 3646–3656
8. M. Lesser, Thirty Years of Liquid Impact Research: A Tutorial Review, *Wear*, 1995, **186–187**, p 28–34
9. M.B. Lesser and J.E. Field, The Impact of Compressible Liquids, *Annu. Rev. Fluid Mech.*, 1983, **15**, p 97–122
10. J.E. Field, J.J. Camusa, M. Tinguely, D. Obreschkowc, and M. Farhat, Cavitation in Impacted Drops and Jets and the Effect on Erosion Damage Thresholds, *Wear*, 2012, **290–291**, p 154–160
11. B.S. Mann, High-Power Diode Laser- Treated HP-HVOF and Twin Wire Arc Sprayed Coatings for Fossil Fuel Power Plants, *J. Mater. Eng. Perform.*, 2013, **22**(8), p 2191–2200
12. B.S. Mann, V. Arya, and B.K. Pant, Cavitation Erosion Behaviour of HPDL-Treated TWAS Coated Ti6Al4V Alloy and its Similarity with Water Droplet Erosion, *J. Mater. Eng. Perform.*, 2012, **21**(6), p 849–853
13. J.I. Cofer, J.K. Reinker, and W.J. Sumner, Advances in Steam Path Technology, GE Power Systems, GER-3713 E
14. E.R. Buchanan, An overview of Erosion Resistant Coatings for Steam Path Surfaces, *Turbo Mach. Int.*, 1987, **28**(1), p 25–28
15. B.S. Mann, Solid Particle Erosion and Protective Layers for Steam Turbine Blading, *Wear*, 1999, **224**, p 8–12
16. B.Q. Wang and M.W. Seitz, Comparison in Behaviour of Iron Base Coatings Sprayed by Three Different Arc Spray Processes, *Wear*, 2001, **250**, p 755–761
17. D.J. Branagan, M. Breitsameter, B.E. Meacham, and V. Belashehenko, High Performance Nano Scale Composite Coating for Boiler Applications, *J. Therm. Spray Technol.*, 2005, **14**(2), p 196–204
18. S. Dallaire, Hard Arc-Sprayed Coatings with Enhanced Erosion and Abrasive Wear Resistance, *J. Therm. Spray Technol.*, 2001, **10**(3), p 511–519
19. P. Georgieva, R. Thorpe, A. Yanski, and S. Seal, Nano Composite Materials: An Innovative Turnover for the Wire Arc Spraying Technology, *Adv. Mater. Process.*, 2006, **164**(8), p 68–69
20. Industrial News, New Benchmark Achieved with the Development of Nanoscale coatings Using Electric Arc Spraying, *J. Therm. Spray Technol.*, 2005, **14**(1), p 13
21. S. Dallaire, H. Levert, and J.G. Legoux, Erosion Resistance of Arc-Sprayed Coatings to Iron Core at 298 K and 588 K, *J. Therm. Spray Technol.*, 2001, **10**(2), p 337–350
22. B.S. Mann and V. Arya, Abrasive and Erosive Wear Characteristics of Plasma Nitriding and HVOF Coatings: Their Application in Hydro Turbines, *Wear*, 2001, **249**, p 354–360
23. B.S. Mann, V. Arya, A.K. Maiti, M.U.B. Rao, and P. Joshi, Corrosion and Erosion Performance of HVOF/TiAlN PVD Coatings and Candidate Materials for High Pressure Gate Valve Application, *Wear*, 2006, **260**, p 75–82
24. B.S. Mann, V. Arya, and P. Joshi, Advanced High-Velocity Oxygen Fuel Coating and Candidate Materials for Protecting LP Steam Turbine Blades Against Droplet Erosion, *J. Mater. Eng. Perform.*, 2005, **14**(4), p 487–494
25. R.J.K. Wood, B.G. Mellor, and M.L. Binfield, Sand Erosion Performance of Detonation Gun Applied Tungsten Carbide/Cobalt–Chromium Coatings, *Wear*, 1997, **211**, p 70–83
26. D.W. Wheeler and R.J.K. Wood, Erosion of Hard Surface Coatings for Use in Offshore Gate Valves, *Wear*, 2005, **258**, p 526–536
27. R.J.K. Wood, Material Selection for Reducing Erosive Damage to Valves, International Conference on Valves and Actuators—Application and Development, Manchester, UK, 1994, p 19–21
28. H.L. de Villiers Lovelock, Powder/Processing/Structure Relationship in WC–CO Thermal Spray Coatings: A Review of Published Literature, *J. Therm. Spray Technol.*, 1998, **7**(3), p 357–373
29. R. Schwetzke and H. Kreye, Microstructure and Properties of Tungsten Carbide Coatings Sprayed with Various High-velocity Oxygen Fuel Spray Systems, *J. Therm. Spray Technol.*, 1999, **8**(3), p 433–438
30. J.A. Browning, Hyper Velocity Impact Fusion- A Technical Note, *J. Therm. Spray Tech.*, 1992, **1**(4), p 289–292
31. H.L. Villiers Lovelock, P.W. Richter, J.M. Benson, and P.M. Young, Parameter Study of HP/HVOF Deposited WC–Co Coatings, *J. Therm. Spray Technol.*, 1998, **7**(1), p 97–107
32. B.S. Mann and V. Arya, HVOF Coating and Surface Treatment for Enhancing Droplet Erosion Resistance of Steam Turbine Blades, *Wear*, 2003, **254**, p 652–667
33. A. Agüero, F. Camón, J.G. de Blas, J.C. del Hoyo, R. Muelas, A. Santaballa, S. Ulargui, and P. Vallés, HVOF-Deposited WC–CoCr as Replacement for Hard Cr in Landing Gear Actuators, *J. Therm. Spray Technol.*, 2011, **20**(6), p 1292–1309
34. B.K. Pant, V. Arya, and B.S. Mann, Enhanced Droplet Erosion Resistance of Laser Treated Nano Structured TWAS and Plasma Ion Nitro-Carburized Coatings for High Rating Steam Turbine Components, *J. Mater. Eng. Perform.*, 2010, **19**(5), p 884–892
35. B.S. Mann, V. Arya, and B.K. Pant, Enhanced Erosion Protection of TWAS Coated Ti6Al4V Alloy Using Boride Bond Coat and Subsequent Laser Treatment, *J. Mater. Eng. Perform.*, 2011, **20**(6), p 932–940
36. B.S. Mann, V. Arya, and B.K. Pant, Influence of Laser Power on the Hardening of Ti6Al4V Low Pressure Steam Turbine Blade Material for Enhancing the Water Droplet Erosion Resistance, *J. Mater. Eng. Perform.*, 2011, **20**(2), p 213–218
37. B.K. Pant, V. Arya, and B.S. Mann, Cavitation Erosion Characteristics of Nitro-carburized and HPDL-Treated Martensitic Stainless Steels, *J. Mater. Eng. Perform.*, 2012, **21**(6), p 1051–1055
38. B.S. Mann, Laser Treatment of Textured X20Cr13 Stainless Steel to Improve Water Droplet Erosion Resistance of LPST Blades and LP Bypass Valves, *J. Mater. Eng. Perform.*, 2013, **22**(12), p 3699–3707
39. J. Grum and R. Sturm, Deformation of Specimen During Laser Surface Remelting, *J. Mater. Eng. Perform.*, 2000, **9**(2), p 138–146
40. B.S. Mann, High-Power Diode Laser Treated 13Cr4Ni Stainless Steel for Hydro Turbines, *J. Mater. Eng. Perform.*, 2014, **23**(6), p 1964–1972
41. S.H. Zhang, J.H. Yoon, M.X. Li, T.Y. Cho, Y.K. Joo, and J.Y. Cho, Influence of CO₂ Laser Heat Treatment on Surface Properties, Electrochemical and Tribological Performance of HVOF Sprayed WC-24%Cr₃C₂-6%Ni Coating, *Mater. Chem. Phys.*, 2010, **119**(3), p 458–464

42. B.S. Mann, Water Droplet Erosion Behavior of High-Power Diode Laser Treated 17Cr4Ni PH Stainless Steel, *J. Mater. Eng. Perform.*, 2014, **23**(5), p 1861–1869
43. S. De Palo, M. Mohanty, H. Marc-Charles, and M. Dorfman, Fracture Toughness of HVOF Sprayed WC–Co Coatings, *Thermal Spray: Surface Engineering via Applications*, Vol 5, 2000, p 245–250